BBAA VI International Colloquium on:
Bluff Bodies Aerodynamics & Applications
Milano, Italy, July, 20-24 2008

NUMERICAL SIMULATION OF THE WIND FLOW AROUND A CUBE IN CHANNEL

Mohammad Omidyeganeh and Jalal Abedi

Department of Chemical and Petroleum Engineering, University of Calgary, 2500 University Drive, NW, Calgary, AB T2N 1N4, Canada
e-mails: momidyeg@ucalgary.ca, jabedi@ucalgary.ca

Keywords: large eddy simulation (LES), Smagorinsky-Lilly sub-grid scale (SGS) model, finite volume (FV) methods, TVD scheme, flow past a cube in channel.

Abstract. *A code has been developed in C++ to solve the Navier-Stokes and continuity equations using large eddy simulation (LES) for the turbulent flow. The finite volume (FV) formulation applied on the staggered grid arrangement for a structured mesh system. Smagorinsky-Lilly sub-grid scale (SGS) model was used which can be substituted with other models easily. The discretisation scheme for all terms except the convection terms, which adopts a TVD scheme, was the central difference scheme. The PISO algorithm had found to be faster than the SIMPLE algorithm for all cases and problems. The laminar flow approaching a cube in the atmosphere boundary layer and in channel was calculated and compared with experiments of turbulent flow. The laminar inflow boundary condition significantly changes the flow pattern around the obstacle. Also the mostly needed modifications had been proposed and estimated.*

1 INTRODUCTION

The wind flow patterns in an urban area strongly affect the dispersion of pollutants around the buildings which is a growing concern in urban environment. The air flow is influenced by various factors, such as the geometry, arrangements of the buildings, the wind directions and the upstream terrain conditions. With a steady growth in computer technology, computational fluid dynamics (CFD) has emerged as an effective tool to establish better understanding of the wind flow around buildings. Nowadays, high performance computing (HPC) provides cluster-based supercomputers for computing applications to make CFD analysis as fast as possible.

CFD codes are structured around numerical algorithms that can tackle fluid flow problems. In order to provide easy user access, most CFD codes include sophisticated input and output interfaces. Hence, they contain three main elements: the pre-processor, the solver, and the post-processor. There are several approaches to computer prediction of flows; the most popular ones involve the use of Reynolds-averaged Navier-Stokes (RANS) equations with a variety of turbulence models. While these are much cheaper than large eddy simulations, no single model has proven capable of predicting a wide variety of complex flows, especially when information about the fluctuating part of the flow is required (Ref. [14]).

These considerations have led to interest in large eddy simulation (LES), in which the large-scale motions are computed explicitly, while the small- or sub-grid-scale motions are modeled. The fundamental rationale behind LES is that large eddies are the ones responsible for most of the mass, momentum and energy transport. These large eddies are strongly dependent on geometry, whereas the smaller eddies are more universal and, thus, easier to model. As the grid resolution increases, the importance of the small eddies diminishes, and LES becomes a direct numerical simulation (DNS). Unfortunately, flows that are of interest to engineering applications (high Reynolds number and complex geometry) are not amenable to DNS, due to prohibitive memory and computational requirements.

The primary objective of our study was the development of a code to investigate the flow past buildings. Most of the applications discussed here are focused on a cube, since it is the simplest idealization of a building and has, therefore, been used most frequently, both in experiments and testing calculation procedures for the flow around buildings.

Castro and Robins in Ref. [1] made the first outstanding effort to obtain a fairly clear picture of the nature of flow in the wake of a surface-mounted cube in uniform and turbulent upstream flows. Theoretical studies of flow around bluff bodies are limited to the description of flow patterns (Ref. [3], Ref. [4], and Ref. [11]). Although the analysis of the flow past 3D bluff bodies has practical importance, quantitative results are scarce; and, very little experimental works have been published on these flows. In 1990, Paterson and Apelt (Ref. [10]) proposed a review of experiments in which turbulent flow over a cube (in a turbulent boundary layer) was studied. However, most of the experiments examined the flow in the vicinity of the cube and measured only a few selected quantities, such as the pressure distribution on the obstacle. The most comprehensive experimental data has been reported by Martinuzzi and Tropea (Ref. [7]) for flow past a cube mounted on a wall of a plane channel at a high Reynolds number.

The processes associated with the flow past structures in the urban boundary layer are so complex and subject to many different parameters. In general, numerical modeling based on

solving the governing partial differential equations, such as momentum, continuity, mass and energy equations, is required for the various flow quantities. Powerful numerical techniques, as well as high capacity computers, are necessary; and, there are various possibilities of treating turbulence in numerical calculations.

Despite progress since the first LES by Deardorff (Ref. [2]), there was not much application of LES to engineering flows for quite a long time, mainly because it requires considerable computing resources and but also due to lack of good models for the small scales. The unsteady turbulent flow field around a cubic model was first simulated by means of LES by Murakami and Mochida (Ref. [8]). Calculations obtained by Rodi (Ref. [12]) with a variety of LES and RANS methods shows that LES is clearly more suited than RANS methods and have great potential for calculating complex flows.

The finite volume (FV) method was adopted to apply LES to the Navier-Stokes equations in the 3D geometry. The code was written entirely in the C++ language except the visualization of the results where the Tec Plot commercial software was used.

2 GOVERNING EQUATIONS

The governing equations consist of the principle of mass conservation and the momentum equations. All quantities were made non-dimensionalized using a length scale H_b (the dimension of the cube) and a velocity scale U_b (the velocity of the laminar flow at the inlet of the domain at the height of the cube).

The filtered continuity and Navier-Stokes equations using the top-hat filter for an incompressible flow are:

$$div(\vec{\bar{u}}) = 0 \tag{1}$$

$$\frac{\partial(\bar{u})}{\partial t} + div\left(\overline{u\vec{u}}\right) = -\frac{\partial \bar{p}}{\partial x} + \frac{1}{\mathrm{Re}} div\left(grad(\bar{u})\right) \tag{2}$$

$$\frac{\partial(\bar{v})}{\partial t} + div\left(\overline{v\vec{u}}\right) = -\frac{\partial \bar{p}}{\partial y} + \frac{1}{\mathrm{Re}} div\left(grad(\bar{v})\right) \tag{3}$$

$$\frac{\partial(\bar{w})}{\partial t} + div\left(\overline{w\vec{u}}\right) = -\frac{\partial \bar{p}}{\partial z} + \frac{1}{\mathrm{Re}} div\left(grad(\bar{w})\right) \tag{4}$$

where u, v, w, P, and Re are the velocities in the x, y, and z-direction, absolute pressure, and Reynolds number ($\mathrm{Re} = \rho U_b H_b / \mu$). For simplicity array notation $\vec{u}$ was used instead of the velocity array. Second terms on the left hand side of Eq. (2)-(4) were treated by defining *sub-grid scale (SGS) stresses*: $\tau_{ij} = \rho\overline{u_i u_j} - \rho\overline{\bar{u}_i \bar{u}_j}$. Smagorinsky (Ref. [15]) suggested that, since the smallest turbulent eddies are almost isotropic, we expect that the Boussinesq hypothesis might provide a good description of the effects of the unresolved eddies on the resolved flow.

$$\tau_{ij} = -2\mu_{SGS}\bar{S}_{ij} + \frac{1}{3}\tau_{ii}\delta_{ij} = -\mu_{SGS}\left(\frac{\partial \bar{u}_i}{\partial x_j} + \frac{\partial \bar{u}_j}{\partial x_i}\right) + \frac{1}{3}\tau_{ii}\delta_{ij} \tag{5}$$

The isotropic part of the SGS stress in Eq. (5) was absorbed into the large scale pressure to avoid dealing with unknown variables and solve them altogether by pressure.

$$\tau_{ij}^{\ a} = \tau_{ij} - \frac{1}{3}\tau_{ii}\delta_{ij} = -\mu_{SGS}\left(\frac{\partial \bar{u}_i}{\partial x_j} + \frac{\partial \bar{u}_j}{\partial x_i}\right) \tag{6}$$

The Smagorinsky-Lilly SGS model builds on Prandtl's mixing-length model and assumes that we can define a kinematic SGS viscosity, $\nu_{SGS} = \mu_{SGS} / \rho$, which can be described in terms of one length scale and one velocity scale. Since the size of the SGS eddies is determined by the details of the filtering function, the obvious choice for the length scale is the filter cutoff width Δ. In 3D computations with grid cells of different length Δx, width Δy and height Δz the cutoff width is often taken to be the cube root of the grid cell volume $\Delta = \sqrt[3]{\Delta x \Delta y \Delta z}$. The velocity scale is expressed as the product of the length scale and the average strain rate of the resolved flow, $\Delta \times \left|\bar{S}\right|$ *where* $\left|\bar{S}\right| = \sqrt{2\bar{S}_{ij}\bar{S}_{ij}}$ and the local rate of strain of the resolved flow are $\bar{S}_{ij} = \frac{1}{2}\left(\frac{\partial \bar{u}_i}{\partial x_j} + \frac{\partial \bar{u}_j}{\partial x_i}\right)$.

$$\mu_{SGS} = \rho\left(C_{SGS}\Delta\right)^2 \left|\bar{S}\right| \tag{7}$$

Different values of C_{SGS} have been imposed so far (Ref. [5] and Ref. [13]); however $C_{SGS}=0.1$ is used more often in the commercial software. The difference in C_{SGS} values is attributable to the effect of the mean flow strain or shear.

3 NUMERICAL METHOD

Simple structured grids are used in this code. Due to the large changes in velocity and pressure next to the wall and around the buildings, refined grids are adopted with a stretch ratio by distance from the walls. A large ratio of grid stretching often leads to numerical oscillation due to the grid size differences between two neighboring grids. The Reynolds number of the flow field treated in atmospheric boundary is usually large which generally requires fine grid resolution. Turbulence modeling makes it possible to use a relatively coarse grid in the domain except near the solid walls of bluff bodies where high prediction accuracy is needed. In order to apply the non-slip boundary condition accurately, it is preferable to set the first grid point below $x_n^+=1$ ($x_n^+ = u^* x_n / \nu$, where u^* is the friction velocity, x_n is the distance from the wall, and ν is kinematic viscosity). For example, in the flow field around a square cylinder (with side length of D) at $Re=22000$ the real length corresponding to $x_n^+=1$ is about $D/1000$ (Ref. [6]).

The code uses a simple stretching procedure where the grid space of an arbitrary grid to the smaller neighbor grid space is equal to the ratio ($\Delta x_n / \Delta x_{n-1} = r$). Thus the number of grids of a distance equal to L with ratio r and the finest resolution dx is given by Eq. (8).

$$n = \left\lfloor \ln\left[1 + L\frac{r-1}{d}\right] \Big/ \ln r \right\rfloor \tag{8}$$

The three dimensional (3D) mesh generated for a cube mounted on a surface is shown in Fig. (1).

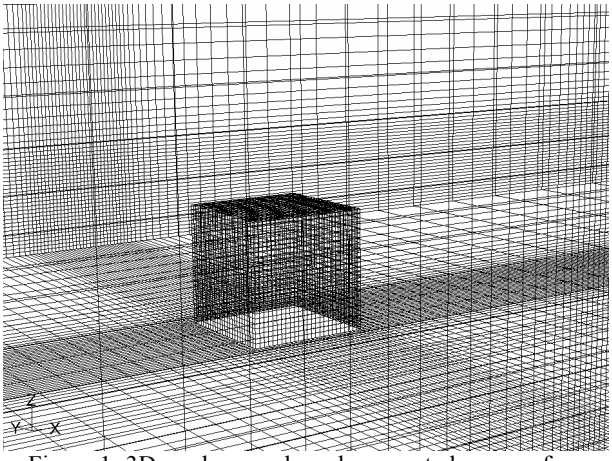

Figure 1: 3D mesh around a cube mounted on a surface

All the equations are discretized based on the finite volume method and a staggered Cartesian grid. In the present research, the code uses second-order accuracy, which means each discretized term in the equation has a truncation error proportional to the square of grid spacing and time marching. This implies that the global truncation error is first-order, and the method is still consistent. Many discretization schemes have been proposed, so far, for the equations that contain convection and diffusion terms the basic upwind scheme is the most stable and unconditionally bounded scheme, but the order of accuracy is low (first-order). Higher order schemes such as central differencing and QUICK can cause oscillations in the results especially when the Peclet number is high. These higher order schemes give unrealistic physical turbulence energy and rates of dissipation (Ref. [16]). Total variation diminishing (TVD) schemes are designed to counteract with the oscillation by adding an artificial diffusion fragment or by adding a weighting towards upstream contribution. Discretization of the diffusion terms in the governing equations using the central differencing is standard and does not require any further consideration.

The general form of TVD schemes of the east face value φ_e is shown in Eq. (9), which uses the notations in Fig. (2) with flow in the positive x-direction.

$$\phi_e = \phi_P + \frac{1}{2}\psi(r)(\phi_E - \phi_P) \tag{9}$$

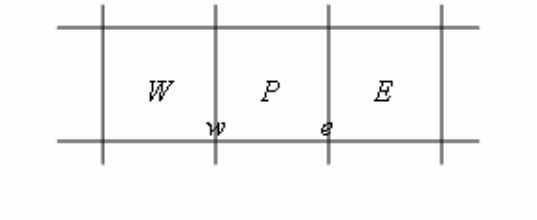

Figure 2: grid notations in the x-direction

where $r = \left(\frac{\phi_P - \phi_W}{\phi_E - \phi_P}\right)$.

By introducing TVD schemes, the goal was to find a stable scheme with a higher-order of accuracy without wiggles. In the present research, due to simplicity, the UMIST function was used.

$$\psi(r) = \max\left[0, \min\left(2r, (1+3r)/4, (3+r)/4, 2\right)\right] \tag{10}$$

Fully implicit method was adopted in the code. Therefore an inner iteration loop was needed to get the accurate results caused by the nonlinearity of the equations. Fully implicit second-order upwind schemes used in the discretization method guarantees the stability of the numerical method. For the time marching term in equations, the Adam-Bashforth second-order scheme was used.

The choice of the time step Δt was governed by several criteria. The stability limit of the time advancement scheme plays no role in this code due to the stable method. However, physical considerations limit the time step selection. In order to predict the turbulence statistics correctly all contributions to turbulence must be resolved and captured. The turbulence fluctuations cannot be satisfied if the computational time step becomes larger than the Kolmogorov time scale (ν/u_τ^2 where u_τ is called frictional velocity). In the present work it was found that the Courant-Fredrichs-Lewy (CFL) limit (shown in Eq. (11)) of *1* produces a time step much smaller than the Kolmogorov time scale.

$$CFL = \Delta t\left(\frac{|u|}{\Delta x} + \frac{|v|}{\Delta y} + \frac{|w|}{\Delta z}\right)_{\max} \tag{11}$$

The no-slip boundary condition was used on all solid walls for all simulations. The free slip boundary condition was used for outflow, where, it was surmised that the length of the domain was long enough that the effect of the bodies are vanished and the fully developed condition was applicable. The symmetry boundary condition was used in the spanwise direction, which, means the normal velocity is zero and the changes in other velocity components are zero.

In wind engineering problems, a high Reynolds number is usually applicable which makes it very difficult to use the no-slip boundary condition at solid walls. Therefore, some wall function should be adopted as a macroscopic boundary condition which is absolutely necessary in this kind of atmosphere problems. Wengle and Werner (Ref. [17]) proposed a wall boundary condition which assumes that at the grid points closest to the wall, the instantaneous velocity components tangential to the wall are in phase with the instantaneous wall shear stress components, and the instantaneous velocity distribution is assumed to follow the linear law of the wall.

$$|\tau_{ub}| = \frac{2\mu|u_P|}{\Delta z} \qquad for \qquad |u_P| \le \frac{\mu}{2\rho\Delta z} A^{\frac{2}{1-B}} \tag{12.a}$$

$$|\tau_{ub}| = \rho\left[\frac{1-B}{2} A^{\frac{1+B}{1-B}}\left(\frac{\mu}{\rho\Delta z}\right)^{1+B} + \frac{1+B}{A}\left(\frac{\mu}{\rho\Delta z}\right)^{B}|u_P|\right]^{\frac{2}{1+B}} \qquad o.w. \tag{12.b}$$

The proposed function was transferred to a non-dimensional form and was used in the code. Δz is the distance of the wall to the closest point in the normal direction, with $A=8.3$ and $B=1/7$. The wall function was not applied explicitly in the equations. Strain calculation uses

this function to get the shear stresses near the walls and implicitly has an interaction in the momentum equations.

Inflow boundary conditions are very challenging since the inlet flow properties are convected downstream, and inaccurate specification of the inflow boundary condition can strongly affect simulation quality. Using an accurate inlet flow was impossible due to lack of exact measurements in real world. One of the most applicable options was to use a non-turbulent mean velocity profile measured experimentally at the inlet. To have a fully turbulent flow at the upstream of the obstacles of a very large domain was required to ensure that the turbulence is fully developed before it reaches the body. This method greatly increases the computational time and was not currently efficient for this code. Another idea was to superimpose random perturbations with the correct turbulence intensity into the mean profile. In the present work the time-averaged streamwise velocity component was set to obey the power law expressed as $z^{1/4}$ in the non-dimensional form (for the half of the channel height where a symmetric profile was adopted for the other half). This expression represents the flow of atmospheric boundary layer conditions while other velocity components are assumed to be zero. The value of ¼ corresponds to the wind tunnel experiment done by Murakami and Mochida (Ref. [9]).

Another problem in turbulent flow simulation is the generation of the initial condition which must contain all the details of the initial three-dimensional velocity field. Since coherent structures are an important component of the flow, it is really difficult to construct such a field. Furthermore, data from experiments or a reliable direct numerical simulation (DNS) are not usually available. The effects of initial conditions are typically remembered by the flow for a considerable time. Thus the initial conditions have a significant effect on the results or at least consume significant computational time to disappear. In the present work there was not such a data for initial conditions and as a result a zero value was used for all variables and a great deal of time was spent to get a reliable results that was not been affected by the initial condition.

The main body of the code was a method that should be used to solve coupled equations in the time step. The most common methods in the literature are SIMPLE, SIMPLER, SIMPLEC, and PISO. The code is capable of switching between the two algorithms SIMPLE and PISO. PISO may be seen as an extended SIMPLE algorithm with one extra corrector step. The PISO algorithm requires additional memory storage due to the second pressure correction equation. It also needs under-relaxation to stabilize the calculation process. Although this method results in significant computational effort in comparison with the SIMPLE algorithm it has been found that the method is fast and efficient. For the present work the central processing unit (CPU) time for a single time step reduced by a factor of 8 compared with the previously discussed standard SIMPLE algorithm.

The selection of solver was changed case by case, and, in the present work SIP (Strongly Implicit Procedure) was used for momentum equations and CG (Conjugate Gradient) for pressure correction equations.

All cases were run on the WestGrid clusters (Glacier and Robson).

4 RESULTS

In the present work, the code described above was used to simulate the air flow around a cube mounted on a surface in channel. The performance of the developed code was examined by comparing the numerical results with the wind tunnel experiments conducted by Martinuzzi and Tropea (Ref. [7]).

The same results as the experimental data were not expected, because the cases used in the simulations were different than reality. The inflow boundary condition plays a major role in the fluid flow characteristics for this kind of problem. Laminar flow as the inflow condition was chosen while the experiments are based on the fully turbulent flow. Zhang (Ref. [18]) showed that the less the upstream turbulence, the larger the cavity size behind the building. This would be resulted in different flow patterns especially behind the cube.

A cube with dimension H_b was mounted on a surface in the computational domain with the streamwise length of $12H_b$, spanwise length of $7H_b$ and height of $2H_b$. The cube was placed $5H_b$ down the inlet and at the middle of the spanwise direction ($3H_b$ distance to each side). The top side boundary condition was changed from the free slip condition for the atmosphere boundary layer into the wall condition for channel flow. Number of meshes was 489,500 and finest grid had dimensions $(0.04H_b,0.04H_b,0.04H_b)$. The stretch ratios of the grids were *1.05* in streamwise and spanwise directions while the grids in z-direction kept unchanged. The Reynolds number based on the cube dimension and inlet streamwise velocity at the height of the cube ($\mathrm{Re} = \frac{\rho U_b H_b}{\mu}$) was *10,000*.

There are plenty of experimental data for the flow past a cube in channel. We compare simulation with the experiments conducted by Martinuzzi and Tropea (Ref. [7]). The differences in the simulation settings are the same as the previous test results such as the inflow condition and the Reynolds number. The experiments conducted for *Re=40,000*. Time-averaged inflow for simulation is compared with experiments in Fig. (3). In addition, time-averaged streamwise velocity profile for several points upstream, top, and behind the cube is illustrated in Figs. (3)-(7). Due to the differences of inflow conditions, the profile of the simulation results should not be the same with the experiments, but the patterns should be the same. A good agreement between the simulations and the experiments were observed.

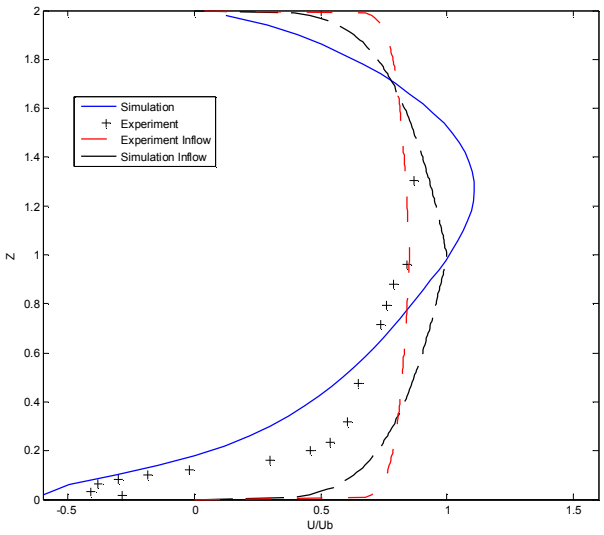

Figure 3: Time-Averaged streamwise velocity at $x=4.58H_b$

In Fig. (4), the flow closes to the cube and as a result streamwise velocity is damped in the lower half. A very good agreement was found on the roof of the cube in Figs. (5) and (6). The negative velocities close to the wall could not be predicted well. Refiner grids next to the wall needed to overcome this inadequacy. Also, the wall treatment affects the flow pattern next to the wall significantly. More investigations on the wall functions are required to result to the best agreement with experiments.

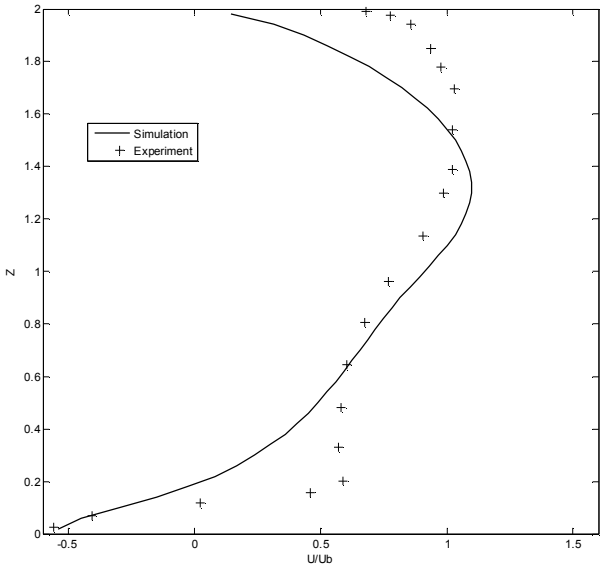

Figure 4: Time-Averaged streamwise velocity at $x=4.68H_b$

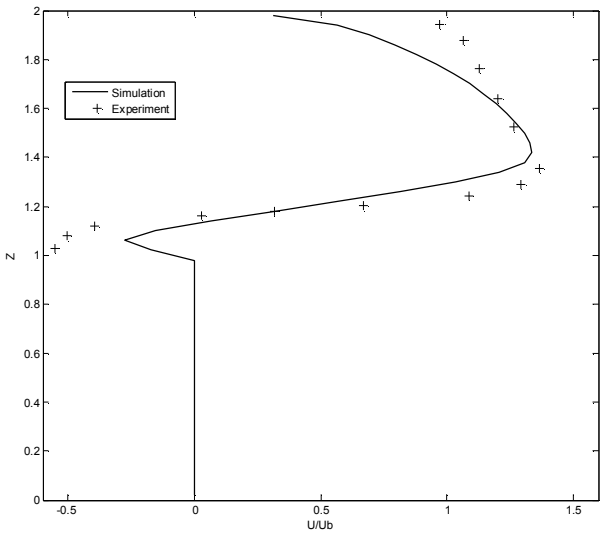

Figure 5: Time-Averaged streamwise velocity at $x=5.5H_b$

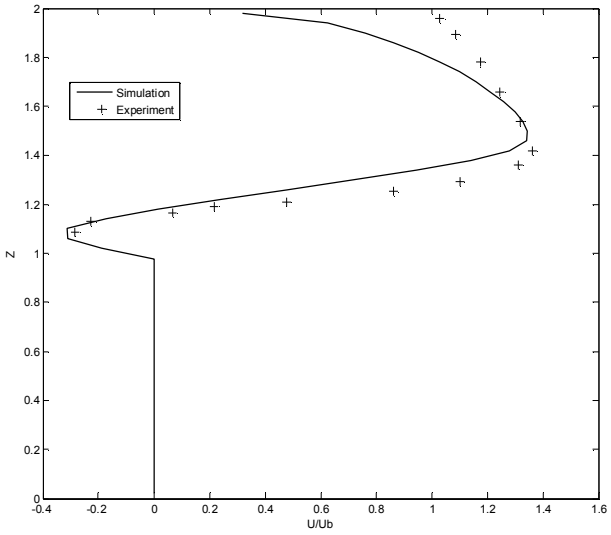

Figure 6: Time-Averaged streamwise velocity at $x=5.75H_b$

Fig. (7) shows the velocity profile behind the cube. The flow pattern differed in lower half of the profile due to the larger vortex behind the cube captured by simulation.

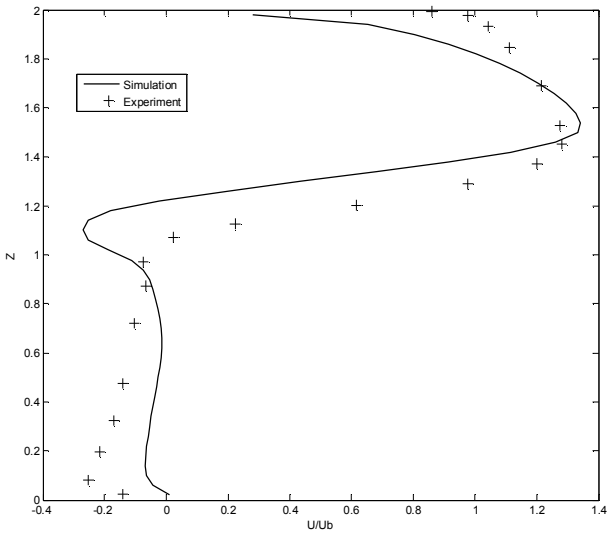

Figure 7: Time-Averaged streamwise velocity at $x=6.08H_b$

Fig. (8) shows that the dimensions of the contours for streamwise velocity are much larger than the experiments. The laminar inflow boundary condition in addition to the SGS model applied in the code cause the larger vortex behind the cube.

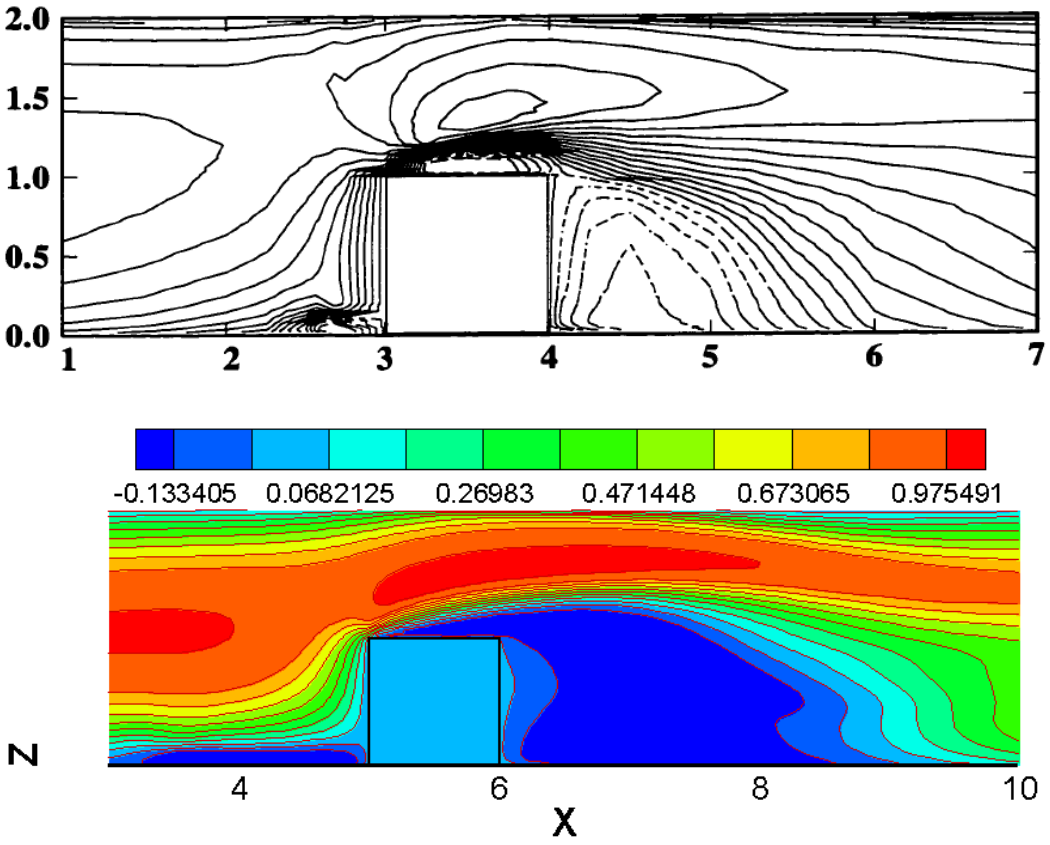

Figure 8: Time-averaged streamwise velocity contours on the symmetry plane. Figure on top is the experimental result of Martinuzzi and Tropea (1993); bottom is the result from LES

The time-averaged streamlines on the symmetry plane for the experiment and simulations are illustrated in Fig. (9). The simulations captured a large vortex behind the building and another in front of the cube on the ground. The vortex on the roof was not captured. The reattachment of the flow behind the building was approximated to be $3H_b$ which was two times bigger than the experiments. However, due to differences in both cases the larger reattachment length was expected for the laminar inflow case.

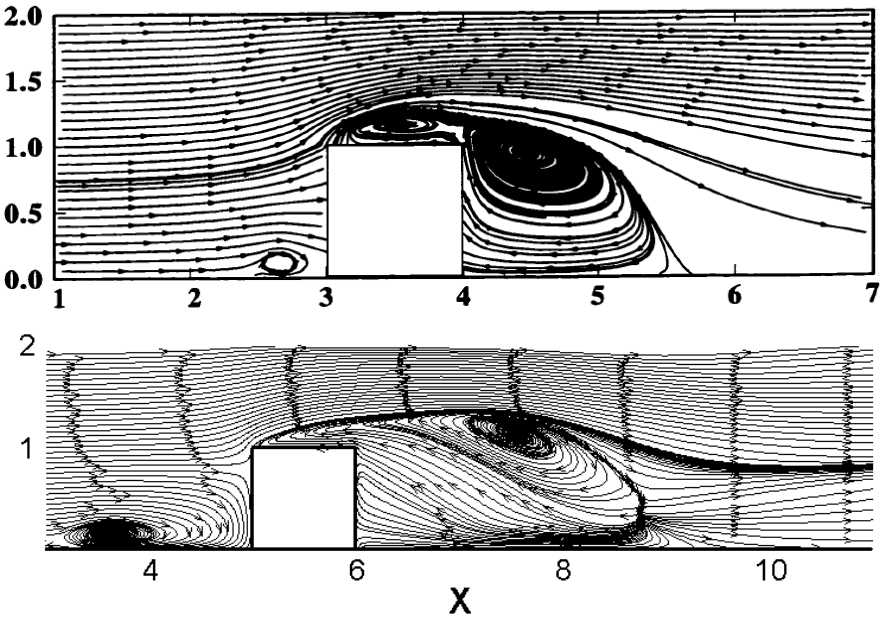

Figure 9: Time-averaged streamlines on the symmetry plane. Figure on top is the experimental result of Martinuzzi and Tropea (1993); bottom is the result of the present code

The profile of the *y*-component velocity resulted by the simulations had a good agreement with the experiments on the roof in Fig. (10). However, the reverse flow on the roof near the corner is under-predicted by the simulations showed in Fig. (11).

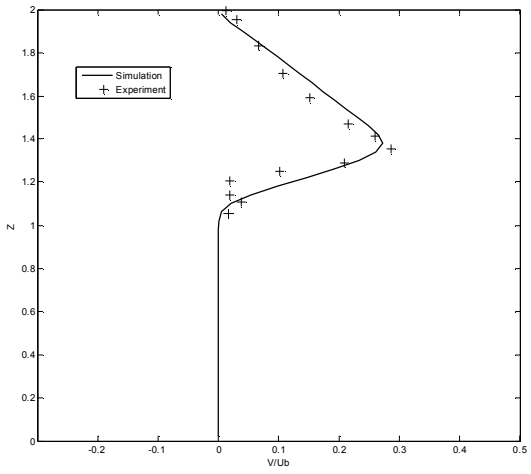

Figure 10: Time-Averaged *y*-component of velocity at $x=5.5H_b$

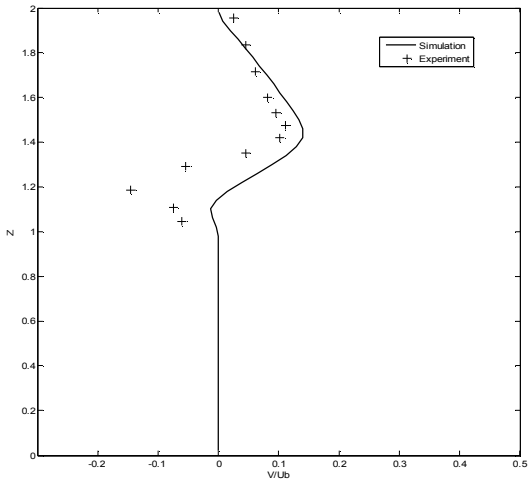

Figure 11: Time-Averaged *y*-component of velocity at $x=5.75H_b$

Despite the flow in the atmosphere boundary layer, here, in channel flow simulations symmetric results were obtained at the horizontal plane of streamlines as shown in Fig. (12).

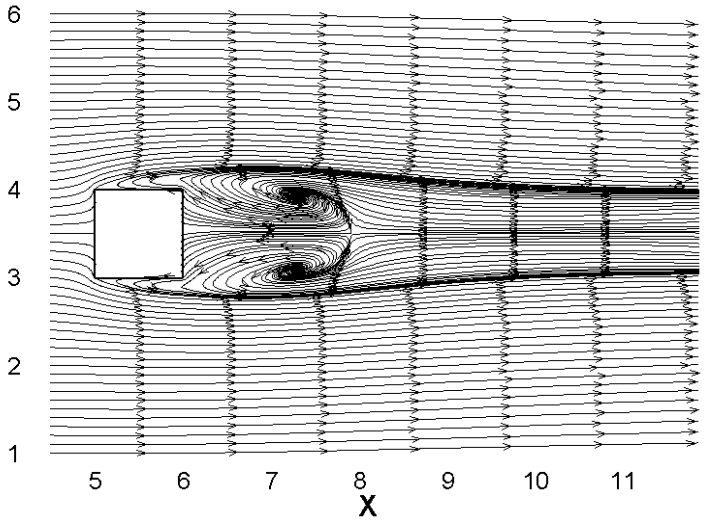

Figure 12: Time-averaged streamlines of flow past a cube in channel at the cube centerline Horizontal plane

One of the most important advantages of LES is the capturing of fluid flow in time. Fig. (13) shows the velocity vectors at the horizontal plane through the center of the cube for different time steps where the vortex shedding was clearly observed.

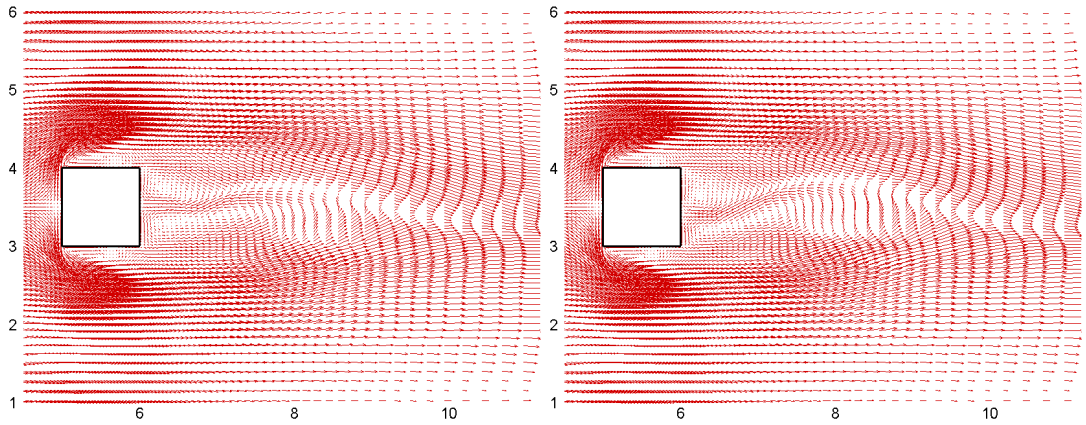

(a) $T=t_0$ (b) $T=t_0+2sec$

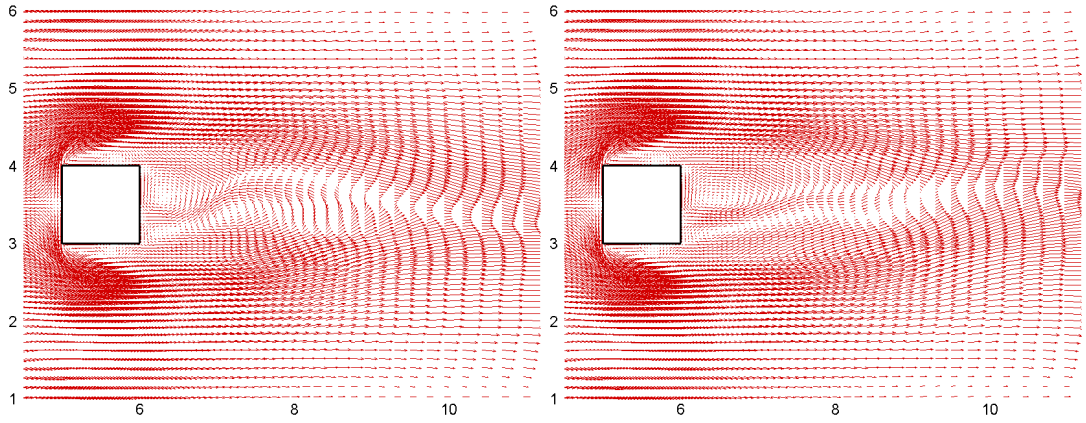

(c) $T=t_0+4sec$ (d) $T=t_0+6sec$

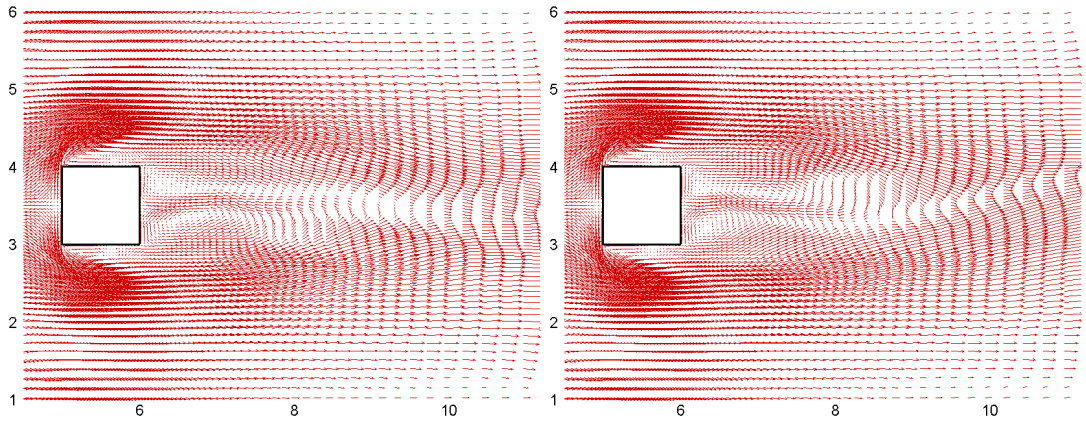

(e) $T=t_0+8sec$ (f) $T=t_0+10sec$

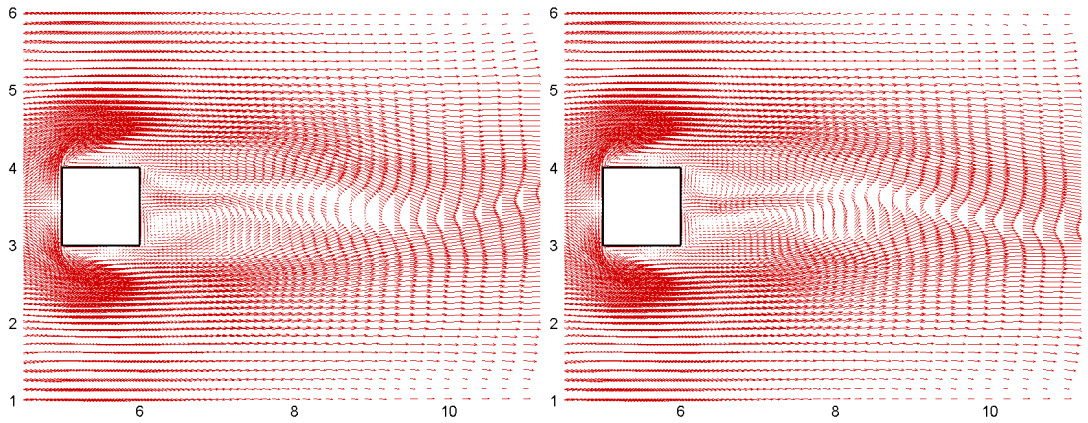

(g) $T=t_0+12sec$ (h) $T=t_0+14sec$

Figure 13: Instantaneous velocity vectors at the horizontal plane through the centerline of the cube at different time steps

5 CONCLUSIONS

It can be concluded from all the results presented above that the developed code in C++ shows a good agreement with the experiments considering the feasible differences due to the non-consistent conditions and settings. The laminar inflow condition in addition to the wall function used in the simulation changed the flow pattern on the roof and behind the cube. No reattachment happened on the roof and a huge vortex appears near the corner of the building. Also, smaller C_s increased turbulence in the flow and decreased the dimension of the vortex behind the building. The channel flow results seem to be more reliable since it is symmetric and concluded that the code solves the flow more accurate.

Due to some limitations exist for the new born code dealing with a 3-D computational domain and turbulent flow, more investigations and modifications are needed to improve the code in an appropriate way. It has been experienced that the first efficient modification would be the acceleration of the code by parallelization. A rapid solution of the equations enables refiner mesh system application. As a result, the convergence criteria could be decreased and relative error definition can be applied. Next step is to investigate all LES models and choose best one to capture flow very well. Applying any other model to the code is too easy since program has been written efficiently and needs adding a new function for the model. There is not any experimental data for the laminar flow at the inlet of the domain and therefore the next step is to find and apply the fully turbulent inlet boundary condition to the simulation. It makes big changes to the results and flow patterns around the cube.

6 ACKNOWLEDGEMENT

This research has been supported by the Natural Sciences and Engineering Research Council of Canada (NSERC) and we are grateful for the financial support. The authors would also like to thank WestGrid Canada for their computational resources.

REFERENCES

[1] Castro I.P, Robins A.G, 'The Flow around a Surface-Mounted Cube in Uniform and Turbulent Streams', Journal of Fluid Mechanics 79, pp 307-335, 1977.

[2] Deardorff J W, 'A numerical study of three-dimensional turbulent channel flow at large Reynolds numbers', Journal of Fluid Mechanic, 41, 453-480, 1970.

[3] Hosker R P Jr., 'Flow and Diffusion near Obstacles', Atmospheric Science and Power Production, edited By Darryl Randerson, Energy Res. Dev. Admin., Washington, DC., 241-326, 1984.

[4] Hunt J C R, Abell C J, Peterka J A, and Woo H, 'Kinematical studies of the Flow around Free or Surface-mounted Obstacles; applying topology of flow visualization', Journal of Fluid Mechanic, 86, 179-200, 1978.

[5] Lilly D.K, 'On the Application of the Eddy Viscosity Concept in the inertial Sub-range of Turbulence', NCAR Report No. 123, 1966.

[6] Lyn D.A, Rodi W, 'The Flapping Shear Layer Formed by Flow Separation from the Forward Corner of a Square Cylinder', Journal of Fluid Mechanics 267, 353, 1994.

[7] Martinuzzi R, Tropea C, 'The flow around surface-mounted, prismatic obstacles placed in a fully developed channel flow', Journal of Fluids Engineering, 115, 85-92, 1993.

[8] Murakami S, Mochida A, 'Three-Dimensional Numerical Simulation of Air Flow around a Cubic Model by Means of Large Eddy Simulation', Journal of Wind Engineering and Industrial Aerodynamics, 25, 291-305, 1987.

[9] Murakami S, Mochida A, '3-D Numerical simulation of the Airflow around a Cubic Model by means of the $\kappa-\varepsilon$ model', Journal of Wind Engineering and Industrial Aerodynamics, 31, 283-303, 1988.

[10] Paterson D A, Apelt C J, 'Simulation of flow past a cube in a turbulent boundary layer', Journal of Wind Engineering and Industrial Aerodynamics, 35, 149-176, 1990.

[11] Perry A E, Chong M S, 'A description of eddying motions and flow patterns using critical-point concepts', Ann. Revs. Fluid Mech., 19 125-155, 1987.

[12] Rodi W, 'Comparison of LES and RANS calculations of the flow around bluff bodies', Journal of Wind Engineering and Industrial Aerodynamics 69-71, 55 75, 1997.

[13] Rogallo R.S, and Moin P, 'Numerical Simulation of Turbulent Flows', *Ann. Rev. Fluid Mech.,* Vol. 16, pp. 99-137, 1998.

[14] Shah K B, 'Large Eddy Simulation of Flow Past a Cubic Obstacle', PhD Thesis, Stanford University, 1998.

[15] Smagorinsky J, 'General Circulation Experiments with the Primitive Equations I. The Basic Experiment', *Mon. Weather Rev.,* Vol. 91, No. 3, pp. 99-164, 1963.

[16] Versteeg H.K, Malalasekera W, 'An Introduction to Computational Fluid Dynamics, the Finite Volume Method', Second Edition, Pearson Education Limited 2000.

[17] Wengle H, Werner H, 'Large Eddy Simulation of Turbulent Flow over and around a Cube in a Plate Channel', Eight Symposium on Turbulent Shear Flows, Technical University of Munich, Sep 9-11, 1991.

[18] Zhang Y Q, 'Numerical Simulation of Flow and Dispersion around Buildings', PhD Thesis, North Carolina State University, 1993.